The Design of Multivariate Field Programs

KENNETH W. JOHNSON

Supercomputer Computations Research Institute, Florida State University, Tallahassee, Florida

(Manuscript received 2 January 1987, in final form 9 September 1987)

ABSTRACT

Development of a methodology for the optimal placement of multivariate sensors as an aid in the design of geophysical field experiments is shown. The optimal placement methodology relies on spatial correlation estimates, interpolation error estimates as provided by a multivariate optimal interpolation scheme, and optimization techniques using nonlinear programming. Atmospheric fields and their associated statistics are simulated by analytic functions to demonstrate the capabilities of the methodology. These include the ability to design new networks, to add sensors optimally to existing networks, and to place restrictions on the region in which sensors can be located by introducing physical and economical constraints on the nonlinear programming problem. It is demonstrated that the mean and variance of the interpolation error for all fields is generally smaller for analyses whose input is derived from optimal sampling locations rather than from subjectively chosen locations.

1. Introduction

The development of strategies in the planning of field programs to make efficient use of limited resources, both physical and financial, while insuring a high probability of successfully sampling the phenomenon of interest is a problem in experimental design. A complete experimental design methodology for the optimal sampling of geophysical phenomena must first determine the geographic and temporal domain most likely to contain the phenomenon of interest. An analysis grid, optimal with respect to size, grid increment, and orientation would need to be found given the region of highest probability of occurrence. Next, decisions regarding the use of a few accurate instruments versus several less accurate instruments would have to be made. Complimentary to the determination of the number of sensors is the problem of optimal siting of the sensors or sample points (in the case of remote sensors). Finally, an archive system, optimal with respect to the data to be collected must be designed. The work described here concentrates on one aspect of the design problem: the determination of optimal sampling point locations.

Optimal sensor placement may be defined as that arrangement of sensors (or sampling points) whose observations, when used in an interpolation scheme or prognostic model, will produce grid point estimates of the sampled fields closer to the true values than any other arrangement of sampling points. Factors influencing this placement include the phenomenon's time/space variability, the chosen analysis grid, and the nature of the observational error. The three primary modes of solution to the experimental design problem in the geophysical sciences have been a statistical approach, an entropy approach, and a dynamical approach. The statistical approach (Gandin, 1963, 1970; Alaka and Elvander, 1972a,b; Myach and Sirotenko, 1973; Eddy, 1974; Seaman, 1977) uses the concepts found in statistical objective analysis, also known as optimal interpolation (Gandin, 1963; Eddy, 1973; Thiebaux, 1973), to produce grid point estimates of mean-squared interpolation error. This technique requires knowledge of the statistical structure of the phenomenon of interest; i.e., the ability to estimate and model the time–space covariances[1] of the fields is a prerequisite. With the use of the estimated covariance functions, optimal interpolation techniques are capable of producing grid point estimates of mean-squared interpolation error. These estimates can be used as an aid in the determination of sensor locations and acceptable observational error limits.

Gandin et al. (1967) and Gandin (1970) used this approach to sensor placement to expand an existing upper air network. His procedure was to compute estimates of mean-squared interpolation error of the existing network. A new observation point was placed at the point of maximum interpolation error. Treating the new observation point as if it already existed, the grid point estimates of interpolation error were recom-

Corresponding author address: Dr. Kenneth W. Johnson, Supercomputer Computations Research Institute, Florida State University, 523 Keen Building, Tallahassee, FL 32306-4052.

[1] The term covariance (correlation) will be used to imply both the autocovariance and cross covariance (correlation) throughout the text.

puted. This procedure was repeated until the maximum mean-squared interpolation error was less than a specified value.

The entropy approach (Husain and Ukayli, 1982; Husain et al., 1984) uses Shannon's entropy concept (Shannon and Weaver, 1949) as found in communication engineering. This concept defines entropy as an average uncertainty consisting of the probability of occurrence of an event. In the case of optimal sensor placement, an event would be a particular meteorological phenomenon of interest. The probabilities associated with a particular phenomenon are computed from long historical records. From these probabilities, entropy may be calculated at each observation point and subsequently interpolated to grid points. This approach was used by Husain et al. (1986) to expand an existing network of surface stations. They computed entropy based on observations from the existing network and placed new stations in the regions of high entropy.

The dynamical approach uses numerical prediction models which simulate the phenomenon of interest. This approach is also known as Observing Systems Simulation Experiments. The earliest users of this method were Alaka and Lewis (1967), Kasahara and Williamson (1972), and the planners of the Global Atmospheric Research Program (GARP; Kasahara, 1972). It attempts to determine the effects of instrumental errors and observational density and frequency upon the growth of errors in prognostic models. The method uses a numerical prediction model to generate a reference atmosphere from a suitable initial reference state. Experimental networks are created by extracting subsets of data from the initial reference state. The numerical model then uses these subsets, with varying degrees of observational error added and suitable initialization, to simulate analysis and forecast cycles. The results of the simulations are compared to the reference atmosphere to determine the effects of the degraded network. The results from such comparisons specify only general network requirements and not specific sampling point locations. Although this approach circumvents the need for knowing the statistical information on the structure and variability of the phenomenon of interest, as in Gandin's approach, or determining the entropy as in Husain's approach, it suffers from the problem of generating a satisfactory reference atmosphere from limited observations. Also, errors inherent in the numerical model, as well as the tendency of different models to produce different results, can have an effect on the design of the experiment.

An improvement to the statistical method of network design is the systems approach. Such an approach has been presented by Myach and Sirotenko (1973), Yerg (1973a,b), and Eddy (1974). In a manner similar to Gandin's, this approach uses the grid point estimates of interpolation error obtained from optimal interpolation schemes as shown by Gandin (1963) and Eddy (1973). Since these estimates are functions only of sampling position when the covariance functions are specified, the interpolation error estimates can be used in stating a criterion for the siting of a network. The problem is then an optimization problem where nonlinear programming techniques can be used to place sensors in a configuration which optimizes the specified criterion. The systems approach to sensor placement permits more flexibility in the design of observational networks than do the dynamical approach using prognostic models or Gandin's approach. A primary feature of the systems approach is the ability to allow economic factors and placement restrictions to enter into the design problem through the use of constraints placed on the nonlinear programming problem.

The systems approach, as Gandin's, relies on the ability to determine the covariance functions of the phenomenon of interest. Buell (1960, 1972) and more recently Julian and Thiebaux (1975) and Thiebaux (1975) have shown some of the requirements and problems in determining and modeling covariance functions for use in interpolation schemes.

A less complex version of the systems approach has been presented by Fujioka (1986). In his application, the true fields at the grid points are known and distance-weighted interpolation is used as opposed to optimal interpolation. The result is a least-squares problem which minimizes the difference between the known true field and the interpolated field as a function of station position. Another variation on the systems approach, as suggested by Bretherton and McWilliams (1980), is the use of entropy in stating a siting criterion which is a function only of sampling positions.

The results presented here are derived from a multivariate version of the systems approach to optimal sensor placement. Atmospheric observations are simulated through the use of analytic functions enabling a comparison to the true fields of analyses made from various network configurations. The application of placement restrictions as constraints on the nonlinear programming problem and the effects on the optimal placement are shown.

2. Sensor placement methodology

The systems approach to optimal placement as presented here is cast as a problem in optimization and is a multivariate extension of the work of Eddy (1974) and Yerg (1973a,b). This approach requires grid point estimates of the mean-squared interpolation errors of multivariate fields. The estimation of such errors is made possible through the techniques of multivariate optimal interpolation. Gandin (1963) proposed the analysis technique with later refinements by Huss (1971), Eddy (1973), Thiebaux (1973), and Schlatter (1975).

The analysis technique used here is similar to the multivariate extension of Gandin's procedure as de-

scribed by Thiebaux (1973). Grid point estimates of a field are obtained by the use of a multivariate, multiple linear regression on irregularly spaced observations. Let $f_{lj} = f_l(x_j, y_j)$ denote the true value of the lth meteorological field at the jth point (x_j, y_j). Also, let $\langle f_{lj} \rangle$ be the ensemble average at (x_j, y_j) of the lth field such that the deviation of the variable from its expected value at (x_j, y_j) is f'_{lj}. The interpolation algorithm estimates the values of the discrepancies from the expected value, $(f_{l0} - \langle f_{l0} \rangle)$, at point (x_0, y_0) by considering a weighted linear combination of the discrepancy values surrounding it, i.e.,

$$\mathbf{F}_0 = Q\mathbf{F} \tag{1}$$

where $\mathbf{F}_0 = [f'_{10}, f'_{20}, \cdots, f'_{L0}]^T$ is the vector of interpolated values for each of the L fields at a given grid point, $\mathbf{F}$ the vector containing the observations of each field from N data points, i.e.,

$$\mathbf{F} = [\mathbf{F}_1{}^T, \mathbf{F}_2{}^T, \cdots, \mathbf{F}_N{}^T]^T;$$

$$\mathbf{F}_j = [f'_{1j} + e_{1j}, f'_{2j} + e_{2j}, \cdots, f'_{Lj} + e_{Lj}]^T$$

and $\mathbf{Q}$ a matrix of unknown weighting factors. Here, e_{lj} denotes the error of observation of the lth field at (x_j, y_j). The superscript T denotes matrix transposition. The unknown weights, Q, are determined by minimizing the mean-square error of interpolation of each field, i.e., the simultaneous minimization of the diagonal elements of E where

$$\begin{aligned} E &= \langle (\mathscr{F}_0 - \mathbf{F}_0)(\mathscr{F}_0 - \mathbf{F}_0)^T \rangle \\ &= \langle (\mathscr{F}_0 - Q\mathbf{F})(\mathscr{F}_0 - Q\mathbf{F})^T \rangle \end{aligned} \tag{2}$$

and $\mathscr{F}_0$ is the vector of the true values at a grid point. The weights which simultaneously minimize the diagonal elements are solutions to the normal equations (Thiebaux, 1973)

$$Q\langle \mathbf{F}\mathbf{F}^T \rangle = \langle \mathscr{F}_0 \mathbf{F}^T \rangle. \tag{3}$$

The matrix $\langle \mathbf{F}\mathbf{F}^T \rangle$ is the spatial autocovariance/cross-covariance matrix of the observational data and $\langle \mathscr{F}_0 \mathbf{F}^T \rangle$ the covariance between the true values at the grid point and the values at the data points.

The mean-squared interpolation error due to optimal interpolation is estimated by the diagonal elements of the matrix:

$$E_{\text{opt}} = \langle \mathscr{F}_0 \mathscr{F}_0{}^T \rangle - \langle \mathscr{F}_0 \mathbf{F}^T \rangle \mathbf{Q}^T. \tag{4}$$

The solution of the sensor placement optimization problem is defined as those space–time coordinates of sampling points which will optimize (minimize or maximize) a stated criterion within a given set of restrictions. When translated into mathematical terms, the criterion to be optimized is termed the objective function. The restrictions act as constraints on the coordinates of the optimally placed sampling points and may be physical or economic in nature.

Several possibilities exist from which to select objective functions. As stated earlier, to add stations optimally to an existing network, Gandin et al. chose to minimize the maximum mean-square interpolation error of the existing network by adding a new station at the point of maximum interpolation error. The objective function chosen by Eddy (1974) and Myach and Sirotenko (1973) consisted of minimizing the weighted mean of the grid point estimates of mean-squared interpolation error for a given field over the sampling volume. Since the sensor placement methodology described here is to apply to multivariate sensor systems, a multivariate analogue to the objective function used by Eddy (1974) was employed.

The multivariate objective function is an expression analogous to (4), obtained when the discrepancy variables are normalized by the standard deviation of the respective fields and used as the interpolation variables in (1), i.e.,

$$\mathscr{E}_{\text{opt}} = \langle \mathscr{F}_0 \mathscr{F}_0{}^T \rangle - \langle \mathscr{F}_0 \mathbf{F}^T \rangle \mathbf{Q}^T. \tag{5}$$

This gives a relation for the relative mean-square interpolation error where $\mathbf{F}$ and $\mathscr{F}$ are vectors of normalized variables and $\langle \mathscr{F}_0 \mathscr{F}_0{}^T \rangle$ and $\langle \mathscr{F}_0 \mathbf{F}^T \rangle$ are now correlation matrices. The elements of $\mathscr{E}_{\text{opt}}$ are dimensionless, the diagonal containing the relative mean-square interpolation errors of the individual fields. Thus, an appropriate multivariate form for the objective function, R, is

$$R = \sum_{l=1}^{L} \sum_{j=1}^{J} \mathscr{E}_{lj}, \tag{6}$$

where $\mathscr{E}_{lj}$ is the lth diagonal element of $\mathscr{E}_{\text{opt}}$ at the jth grid point. As seen in (5), estimates of $\mathscr{E}_{\text{opt}}$ are a by-product of the optimal interpolation technique. Given the ability to specify correlations at any spatial lag and the statistical character of the observational errors, (5) becomes a function of the location of the sampling points only. No observational data are required in the evaluation of (6).

The computational procedure for determining the optimal locations of the sampling points relies on the optimization techniques of nonlinear programming. Nonlinear programming is a branch of mathematical programming which allows for the solution of optimization problems of the form

$$\min_{\mathbf{x}} \{R(\mathbf{x})\}; \quad \mathbf{x} \in E^N$$

subject to

$$\begin{aligned} H_j(\mathbf{x}) &= 0; \quad j = 1(1)n \\ G_j(\mathbf{x}) &\geqslant 0; \quad j = 1(1)p \end{aligned} \tag{7}$$

where $\mathbf{x}$ is a column vector in N-dimensional Euclidean space, E^N. The functions $R(\mathbf{x})$, $H_j(\mathbf{x})$, and $G_j(\mathbf{x})$ represent the objective function, the n equality constraints, and the p inequality constraints, respectively. These may be either linear or nonlinear. For the problem of optimal sampling, R is an objective function as de-

scribed by (6). The functions G and H can be either physical or logistical constraints placed on the number and location of the sampling points. The coordinates of the sampling points in a space–time volume are contained in the N-vector $\mathbf{x} = [x_1, y_1, z_1, t_1, \cdots, x_K, y_K, z_K, t_K]^T$ where K is the number of sampling points and $N = 4K$. The variable N is reduced appropriately if the sampling and analysis domain is not four-dimensional.

The nonlinear programming technique used here is described by Himmelblau (1972) and is known as the flexible tolerance method. This is an iterative direct search method as opposed to derivative methods which require analytic forms of the first and possibly second derivatives of the objective function. An initial guess of the optimal solution termed the starting vector is required to initiate this procedure. The advantages of using the flexible tolerance technique to determine sampling point locations depend principally on the fact that it is an easily implemented direct search method. This technique is constructed to avoid premature termination of the search at a nonlocal optimum. Also, since this technique forces the satisfaction of any constraints that might be applied to the problem to improve as the search progresses toward the solution, there is little chance that the constraints will not be satisfied when a solution is obtained. Other nonlinear programming techniques may be applicable to the sensor placement problem. However, since the exploration of nonlinear programming algorithms is not the primary purpose of this work and the flexible tolerance method was readily available, other methods were not considered.

The flexible tolerance technique, as is true for any other nonlinear optimization technique, is not guaranteed to converge to the global optimum if several local optima are present. Which local optimum the method converges to usually depends upon the choice of starting vector. The likelihood of the presence of several local optima in the sensor placement problem increases as the complexity of the objective function increases and the number of sampling points increases. Determination of locally optimum solutions can be achieved by solving the placement problem with several different initial sampling point configurations (starting vectors). The optimal configuration as defined here is the one that produces the smallest objective function value regardless of the initial configuration.

3. Analytic fields

The testing and evaluation of the sensor placement algorithm and the accompanying optimal interpolation scheme employed analytic functions to simulate multivariate atmospheric phenomenon and their associated correlation functions. Use of the placement methodology requires knowledge of the spatial correlation functions of the relevant multivariate fields. Similarly, the optimal interpolation scheme requires knowledge of the spatial correlations in addition to observational data. Data collected in the atmosphere are typically contaminated by instrumental errors and aliasing of small scales. Thus, the true values, either at grid points or at sampling points, are never known. For this reason, real data with its associated errors were judged inadequate in evaluating the placement methodology.

The analytic model used to simulate atmospheric fields relied on the constraint of geostrophy to generate values representative of the multivariate fields of geopotential, Φ, and the x and y components of the wind, u and v, respectively. The functions representing the geostrophic fields are

$$\left.\begin{aligned} \Phi_j &= \Phi(x_j, y_j) = A\cos(\omega_x X_j)\cos(\omega_y Y_j) - BY_j \\ u_j &= u(x_j, y_j) = \frac{1}{f_j}\left[A\omega_y \cos(\omega_x X_j)\sin(\omega_y Y_j) + B\right] \\ v_j &= v(x_j, y_j) = -\frac{1}{f_j} A\omega_x \sin(\omega_x X_j)\cos(\omega_y Y_j) \end{aligned}\right\} \tag{8}$$

where

$$X_j = x_j - x_c$$

$$Y_j = y_j - y_c$$

$$(x_j, y_j) = \text{coordinates of the } j\text{th point}$$

$$\omega_x = \frac{2\pi}{l_x}, \quad \omega_y = \frac{2\pi}{l_y}.$$

Here, in the x direction, x_c, ω_x, l_x are the origin of the system, the radian wavenumber, and the wavelength, respectively. The variables y_c, ω_y and l_y are similar quantities in the y direction. The variables A, B, ω_x and ω_y are assumed to be random variables with independent normal distributions. Under these assumptions the expected value of the fields and the spatial covariances among the Φ, u and v fields can be derived. These are given in the Appendix. A realization of the Φ, u and v fields is shown in Figs. 1–3. The fields shown are a single realization resulting from the random drawing of A, B, ω_x and ω_y from independent normal distributions. The spatial correlation functions associated with (8) were evaluated by normalizing the covariance expressions by the appropriate standard deviations. The correlations are shown in Fig. 4 where the zero-lag reference point is taken at the center of the grids shown in Figs. 1–3. The mean and variance associated with analytic fields are spatially inhomogeneous and the correlation functions anisotropic. Since homogeneity of the statistics is the usual assumption when considering atmospheric statistics, the analytic model presented here provides an adequate test field for the analysis and placement algorithms. The analytic fields chosen here, as well as their associated statistics, are time independent, i.e., they are

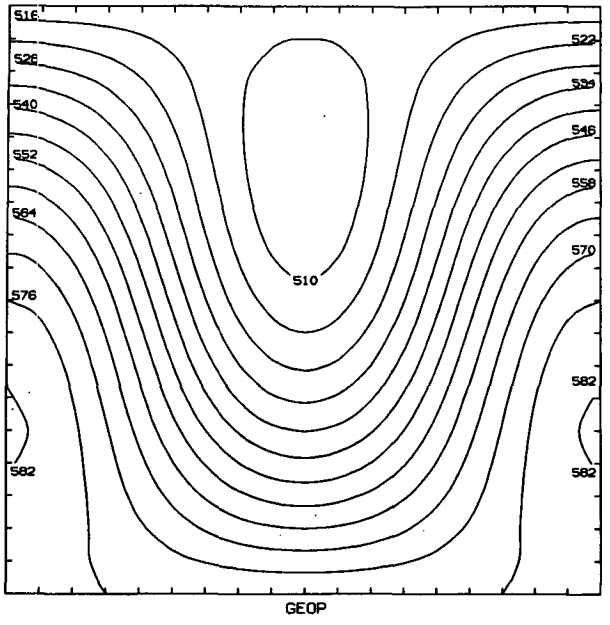

FIG. 1. Geopotential field (10^2 m^2 s^{-2}) as computed from Eq. (8).

functions of (x, y) only. Although a time dependency could be included in the functional form of the equations which would allow each realization to evolve in time, that would add another level of complexity which is not relevant to the primary purpose of this work. With the addition of time as an independent variable, the optimal (x, y, t) for an observation point would need to be determined. This would require time/space correlations to be employed by the placement algorithm in a manner analogous to that presented by Huss (1971) for optimal interpolation using off-time data. Although the placement methodology is sufficiently general to accommodate the time dependency, that aspect was not explored in this work.

4. Evaluation of sensor placement methodology

Several numerical experiments were performed in an effort to evaluate the capabilities of the sensor placement methodology. These experiments used the analytic fields presented earlier, in multivariate and univariate form, as truth in order to compare objectively analyzed fields derived from subjectively and optimally placed sampling points. The evaluation compared the effects of optimal sensor placement upon the mean and variance of the interpolation error and compared the differences between univariate and multivariate sensor placement and analysis. Five starting vectors were used, each consisting of a set of 15 randomly determined sampling point coordinates. For each starting vector, four sensor placements were performed: one multivariate placement and one univariate placement for each of the three analytic fields. All experiments were performed on the 7×7 grid shown in Figs. 1–3 with an influence radius large enough to include all 15 sampling points at every grid point. Since the data were generated from the analytic model and its associated correlation functions there were no sources of error in the objective analyses from either the data or the correlations.

The univariate sensor placement experiments used the objective function given by (6) with $l = 1$. It was assumed in the univariate experiments that each of the three fields would be sampled separately and independently of each other. Thus, the placement algorithm required only the autocorrelation function for the field being sampled. The multivariate sensor placement experiments used the objective function given by (6) and assumed multivariate samples to be taken at each sampling point. The multivariate sensor placement experiments required the complete set of autocorrelations and cross correlations associated with the analytic fields.

The effectiveness of the sensor placement methodology was evaluated by comparing the mean and variance of the interpolation error arising from analyses using sensors at the initial locations to analyses using sensors at the final locations. The initial and final positions of the sensors for starting vector 1 are shown in Figs. 5–8 for the univariate and multivariate experiments. Tables 1–5 give the results of the objective analyses performed on data generated at the initial and final locations for all five starting vectors. Columns 3 and 5 of Tables 1–5 show a general decrease in the mean interpolation error when the optimal locations

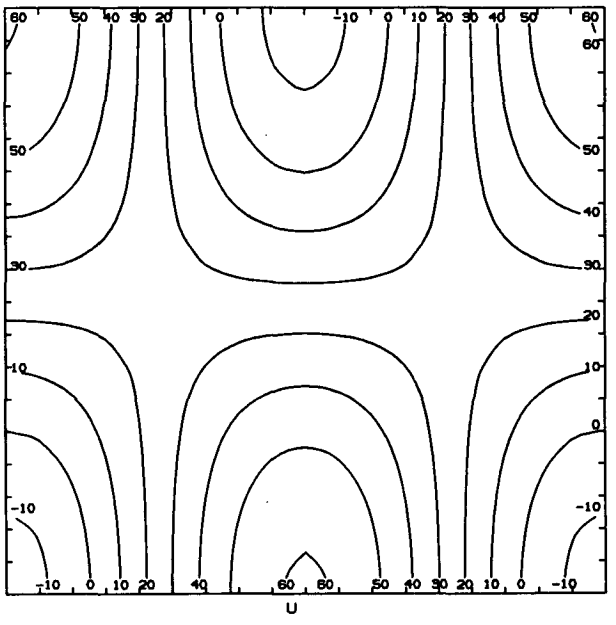

FIG. 2. As in Fig. 1 except for x-component of wind field (m s^{-1}) as computed from Eq. (8).

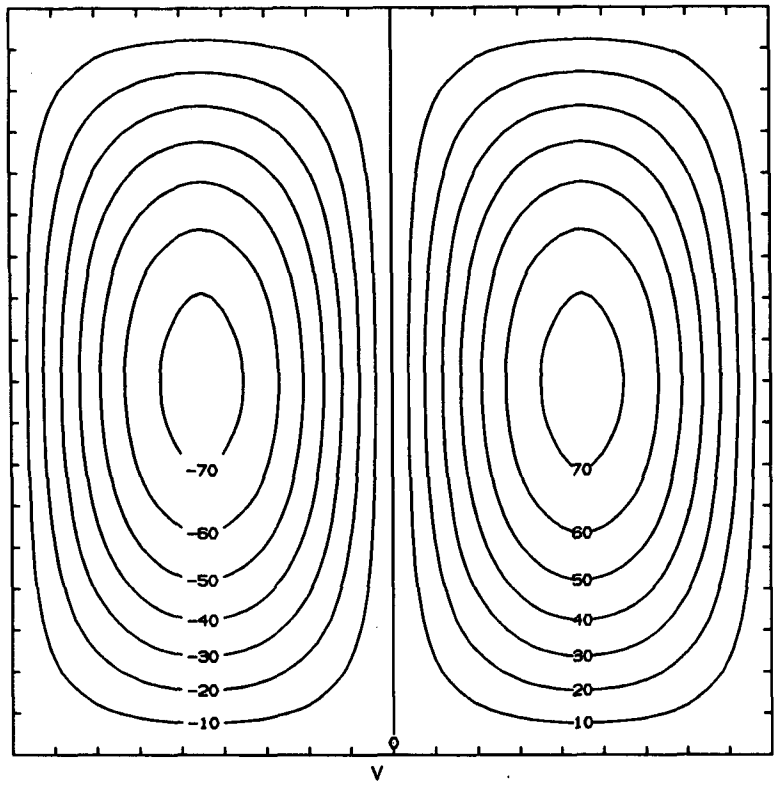

FIG. 3. As in Fig. 1 except for y-component of wind field (m s^{-1}) as computed from Eq. (8).

were used as sampling points. A few exceptions to this can be seen in the u and v fields; however, the increase is generally small.

The variance of the interpolation errors for the analyses using the optimal sampling locations also shows a general decrease over the errors resulting from analyses using the initial sampling points. This is seen in columns 4 and 6 of Tables 1–5. As with the mean interpolation error, four of these cases show small increases in the variance of the interpolation error.

Several possible factors could account for the increase in the mean and variance of the interpolation error. The most important relates to the fact that the theoretical development of optimal interpolation and, hence, of the optimal placement is based upon ensemble averages. Thus, it is possible that when considering specific realizations of an event, as was done here in evaluating the placements, the sensor placement could be suboptimal with respect to a particular realization. However, when evaluated over an ensemble the placement would be optimal.

An evaluation of multivariate versus univariate placement shows that for all fields, regardless of the starting vector, the multivariate placement was superior when judged by the reduction in the mean and variance of the interpolation error.

A by-product of these experiments is the opportunity to compare univariate and multivariate analyses. Comparisons made from Tables 1–5 of the univariate versus multivariate optimal interpolation for the initial positions show that in all but two cases, the multivariate interpolation produced analyses with mean and variance of interpolation error that was significantly smaller than its univariate counterpart. This illustrates the effect that different correlated fields can make in the analysis of one another. A similar comparison dealing with this effect alone and using the final positions could not be made since the final positions for each of the univariate experiments were different from the final positions of the multivariate experiments.

The final two experiments discussed here placed constraints on the admissible locations of the sampling points; otherwise these experiments were identical to the multivariate experiment using starting vector 1. These results are shown in Table 6 and Figs. 9 and 10. The first of these experiments, experiment 21, used starting vector 1 but assumed three of the 15 sensors were fixed and not subject to optimal placement although their influence upon the placement of the other sampling points was allowed. This type of constraint would be useful when adding sensors to an existing fixed network. The fixed sensors are indicated in Fig. 9 by squares. The numerical results are shown in Table 6. The most notable difference between the results of

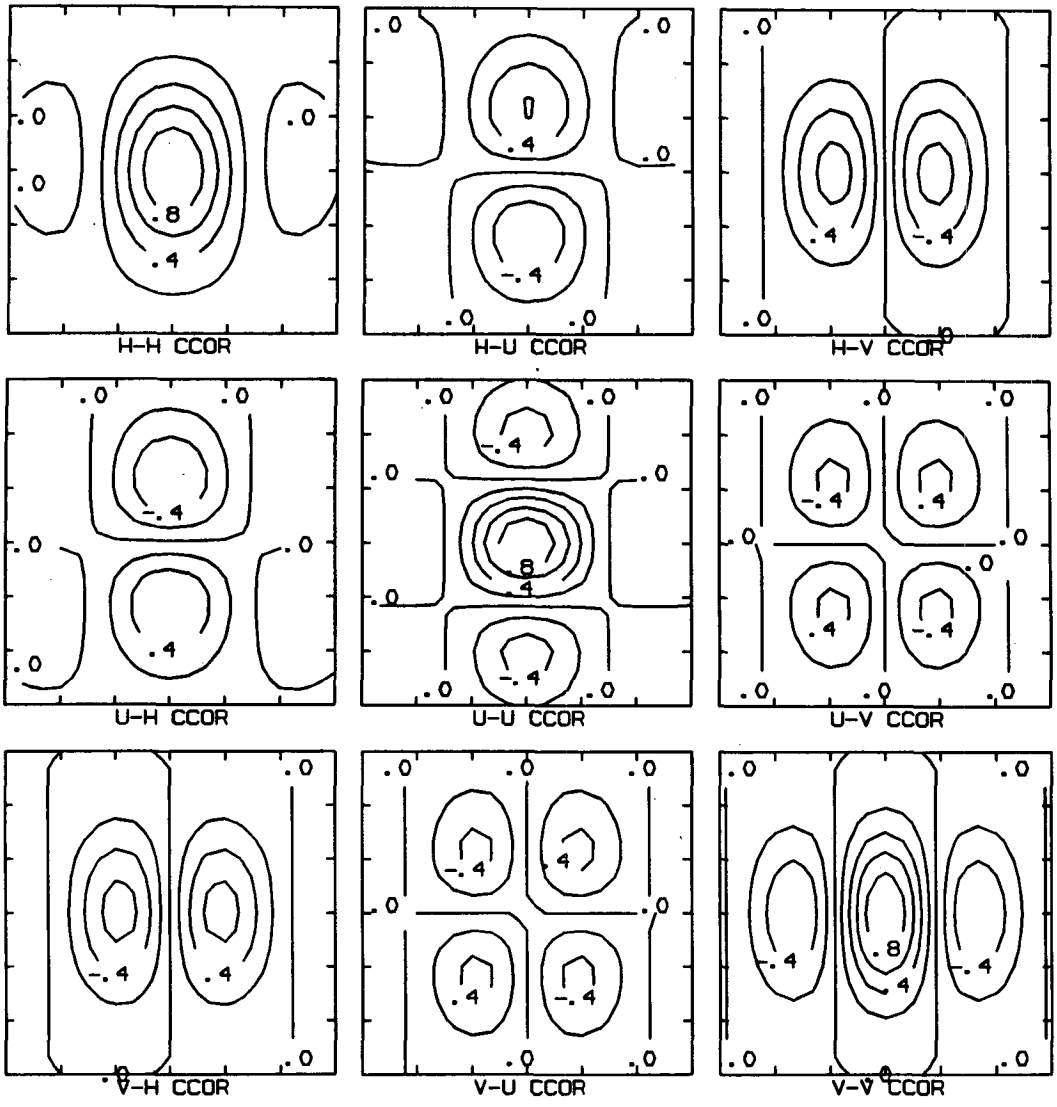

FIG. 4. Spatial autocorrelation and cross correlations among the variables Φ, u and v as computed from the analytic covariance relations in the Appendix. Zero-lag reference point is at center of grid shown in Fig. 1.

the unconstrained experiment and experiment 21 was in the final locations of sensors 13 and 3. Of the three fixed sensors, sensors 4 and 11 were relocated by the greatest distance in experiment 4 and the sensors immediately surrounding 4 and 11 are most affected by the constraint that 4, 11 and 12 remain fixed. The mean and variance of the interpolation error are smaller than the subjectively placed sensors. When compared to the unconstrained multivariate placement the fixed station placement does not seem to produce analyses significantly better or worse than the unconstrained multivariate case. For example, the geopotential is better sampled by the constrained placement when considering the mean of the interpolation error but produces a worse analysis when considering the variance of the interpolation error. This can be explained by the fact that the objective function considers the interpolation errors of all fields averaged together as opposed to minimizing the errors of the fields independently. Constraining the placement could lead to an improvement in the analysis for one particular field but not in the others when compared to the unconstrained multivariate case. In general, a constrained sensor placement will be suboptimal when compared to an unconstrained placement.

The final experiment, No. 22, placed restrictions on the regions of the grid that were admissible for final sensor placement. These restrictions were introduced into the problem mathematically as equality and inequality constraints placed on the nonlinear programming problem. One equality and two inequality constraints were used in this experiment. The equality

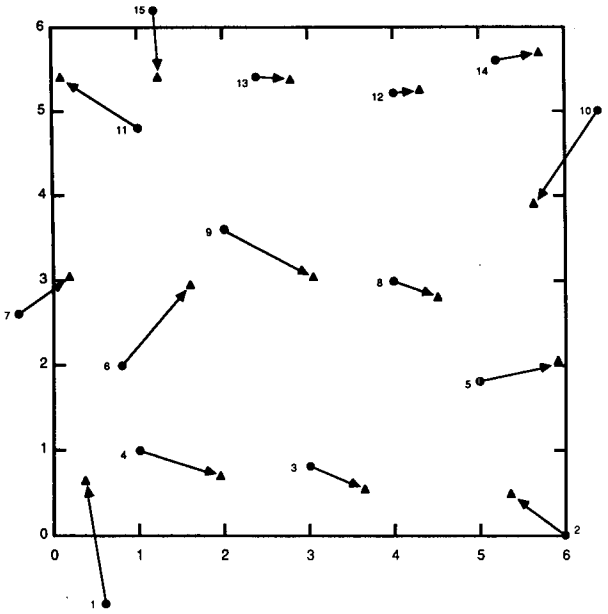

FIG. 5. Optimum deployment of sensors for the univariate sampling of geopotential as determined by the sensor placement algorithm using starting vector 1. Dots indicate initial locations (starting vector) and triangles indicate final location (solution vector).

constraint described a straight line upon which specified sensors were to be placed. The line is represented by the equation

$$y - 2x + 5.2 = 0 \qquad (9)$$

and is shown in Fig. 10. The first inequality constraint described a region outside of which specified sensors could not be placed. Such a constraint might be useful when optimally placing automated remote stations that must be within communication range of a base station. This constraint described the area within a circle and was represented by

$$(1.05)^2 - (x - 1.9)^2 - (y - 4.6)^2 \geq 0. \qquad (10)$$

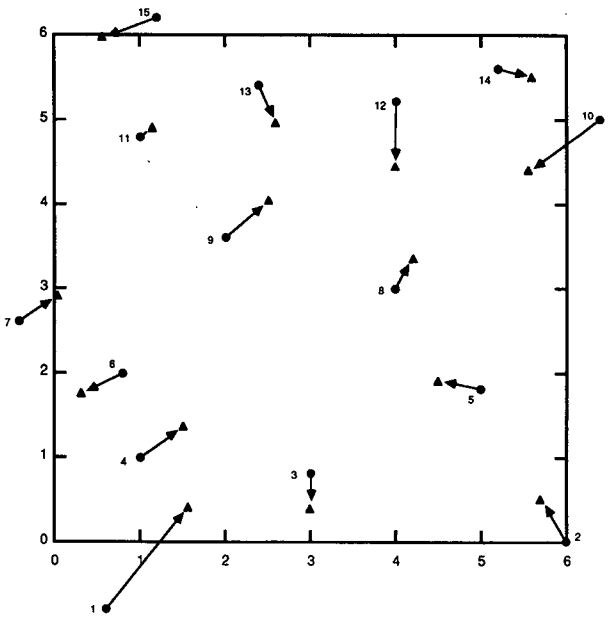

FIG. 6. As in Fig. 5 except for x-component of wind.

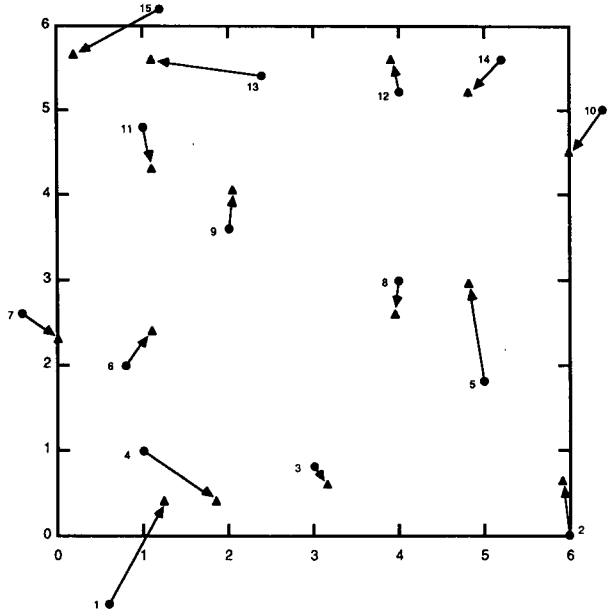

FIG. 7. As in Fig. 5 except for y-component of wind.

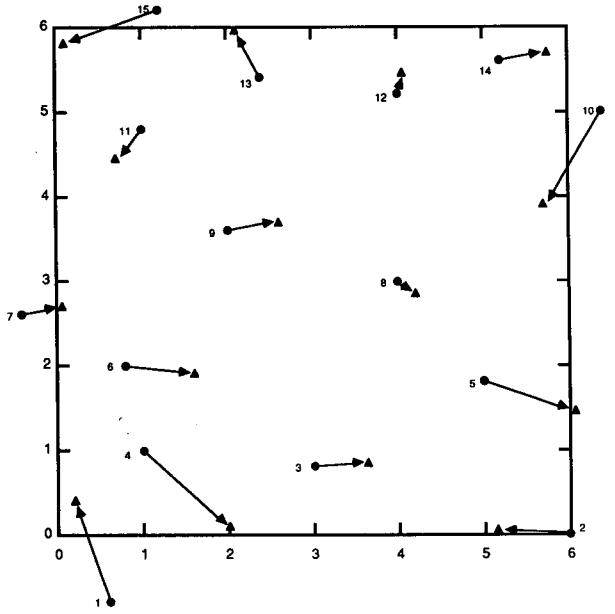

FIG. 8. Optimum deployment of sensors for the simultaneous multivariate sampling of geopotential and wind components as determined by the sensor placement algorithm using starting vector 1.

TABLE 1. Mean and variance of analysis error for sensor placement using starting vector 1.

	Expt No.	Field	Initial positions: Mean of error	Initial positions: Variance of error	Final positions: Mean of error	Final positions: Variance of error	Objective function: Initial	Objective function: Final
Univariate	1	Φ	186.70	514400	44.63	96420	17.93	12.48
	2	u	1.28	165	−0.70	179	26.09	21.33
	3	v	0.72	352	0.71	182	25.55	15.55
Multivariate	4	Φ	116.40	57670	13.45	4806	4.12	1.13
	4	u	0.67	41	−0.08	19	9.12	5.24
	4	v	0.98	48	−0.09	14	6.21	3.37

TABLE 2. As in Table 1 except for starting vector 2.

	Expt No.	Field	Initial positions: Mean of error	Initial positions: Variance of error	Final positions: Mean of error	Final positions: Variance of error	Objective function: Initial	Objective function: Final
Univariate	5	Φ	124.50	909200	42.46	125000	21.17	12.23
	6	u	1.07	332	−0.50	188	28.24	21.24
	7	v	0.08	420	2.42	413	22.79	16.29
Multivariate	8	Φ	69.15	84670	−6.69	3641	5.85	1.27
	8	u	−0.89	54	0.32	18	10.52	5.48
	8	v	1.68	34	0.01	9	7.85	3.36

TABLE 3. As in Table 1 except for starting vector 3.

	Expt No.	Field	Initial positions: Mean of error	Initial positions: Variance of error	Final positions: Mean of error	Final positions: Variance of error	Objective function: Initial	Objective function: Final
Univariate	9	Φ	180.70	356400	20.05	122400	16.48	12.58
	10	u	0.66	199	−2.05	172	25.70	21.55
	11	v	−1.53	320	−0.78	297	23.31	16.01
Multivariate	12	Φ	46.02	29550	4.50	6147	2.69	1.17
	12	u	−0.59	35	0.31	18	7.38	5.03
	12	v	−0.81	34	−0.46	14	5.76	3.20

TABLE 4. As in Table 1 except for starting vector 4.

	Expt No.	Field	Initial positions: Mean of error	Initial positions: Variance of error	Final positions: Mean of error	Final positions: Variance of error	Objective function: Initial	Objective function: Final
Univariate	13	Φ	107.70	178700	15.52	11700	14.80	12.39
	14	u	−1.20	149	−1.48	169	25.69	21.70
	15	v	1.16	157	0.39	235	22.15	16.50
Multivariate	16	Φ	40.41	15760	0.62	5272	2.26	1.16
	16	u	0.69	28	0.23	19	6.87	5.03
	16	v	0.88	42	0.43	9	5.88	3.14

TABLE 5. As in Table 1 except for starting vector 5.

	Expt No.	Field	Initial positions: Mean of error	Initial positions: Variance of error	Final positions: Mean of error	Final positions: Variance of error	Objective function: Initial	Objective function: Final
Univariate	17	Φ	244.00	520500	22.96	142500	16.70	12.87
	18	u	1.20	208	−0.01	162	24.98	20.92
	19	v	0.39	249	−1.13	331	21.45	16.95
Multivariate	20	Φ	102.50	96070	5.26	6071	3.68	1.38
	20	u	0.00	47	0.15	21	7.18	5.18
	20	v	−0.01	91	0.05	16	6.37	3.30

The restricted region is the circle shown in Fig. 10. In this case, the three sensors were optimally placed within the confines of the circle.

The second inequality constraint described a region inside of which specified sensors could not be placed. Constraints of this type are useful to prevent placement of sensors in undesirable regions such as bodies of water. The constraint was

$$25.0(x - 1.9)^2 + 6.25(y - 2.0)^2 - 1.0 \geq 0 \quad (11)$$

and describes the ellipse shown in Fig. 10. This experiment used the same starting vector as experiment 4. The constraints of this experiment were chosen such that the final positions of several of the sensors in experiment 4 violated these constraints. Figure 10 shows the initial and final positions for this experiment. As seen in this figure, none of the final locations violates the constraints. The final positions are optimal with regard to these constraints and the stated optimization criterion as indicated by the decrease in the objective function. Table 6 indicates that the cost for satisfaction of the constraints is possibly a poorer analysis when compared to the unconstrained case. As seen in Table 6, certain error statistics for certain fields appear to be better for the constrained case as opposed to the unconstrained case; however, the argument presented for the fixed sensor case regarding these statistics applies here as well. The fact still remains that the constrained but optimally determined sensor locations yield analyses that have smaller mean and variance of interpolation error than the subjectively chosen locations.

Optimal interpolation, and consequently the sensor placement methodology, is capable of accounting for observational error. This error may be incorporated into the sensor placement methodology in a statistical sense through the correlation matrix. For the case of

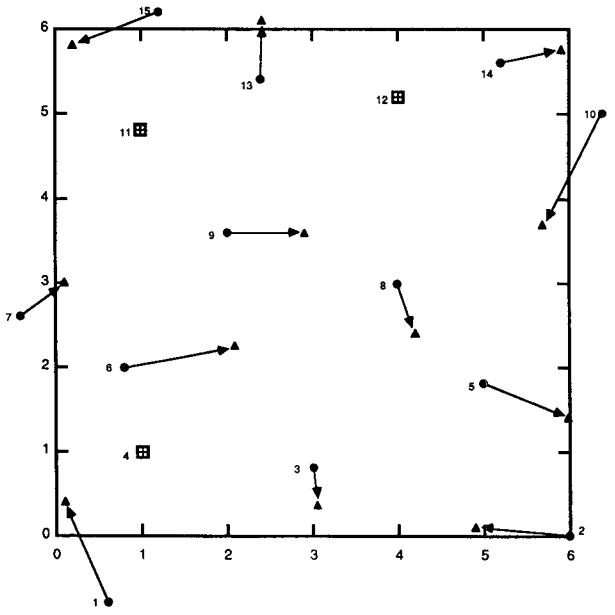

FIG. 9. As in Fig. 8 except sensors 4, 11 and 12 are treated as existing fixed sites.

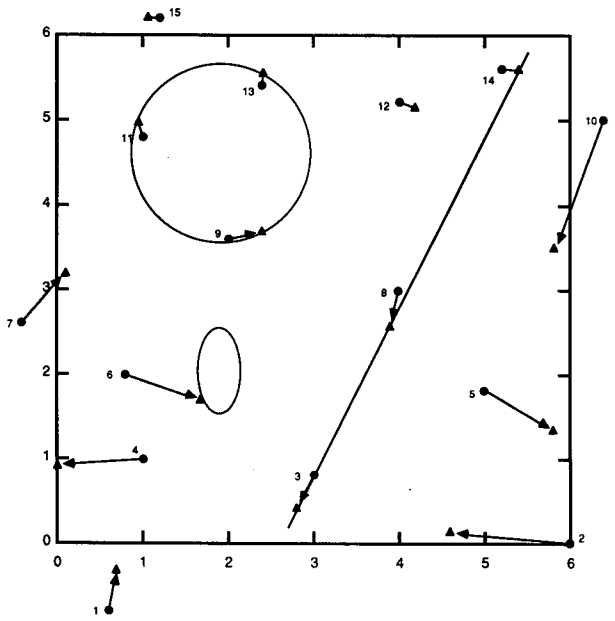

FIG. 10. As in Fig. 8 except sensors 9, 11 and 13 are constrained to remain inside the circle; sensors 3, 8 and 14 are constrained to remain on the straight line segment and all sensors are constrained to remain outside of the elliptic area.

TABLE 6. As in Table 1 except for starting vector 6.

	Expt No.	Field	Initial positions: Mean of error	Initial positions: Variance of error	Final positions: Mean of error	Final positions: Variance of error	Objective function: Initial	Objective function: Final
	4	Φ	116.40	57670	13.45	4806	4.12	1.13
	4	u	0.67	41	−0.80	19	9.12	5.24
	4	v	0.99	48	−0.09	142	6.21	3.37
Fixed	21	Φ	116.40	57670	11.16	5177	4.12	1.43
	21	u	0.67	41	−0.35	14	9.12	5.73
	21	v	0.99	48	−0.11	11	6.21	4.35
Constrained	22	Φ	116.40	57670	1.44	7728	4.12	1.78
	22	u	0.67	41	−0.21	29	9.12	6.04
	22	v	0.99	48	−0.34	11	6.21	3.08

uncorrelated observational errors, the relative error (the ratio of the observational error variance of a field to the field variance) is added to the diagonal of the correlation matrix, $\langle \mathbf{F}\mathbf{F}^T \rangle$, used to determine the weights Q as shown by Schlatter (1975). Observational errors, correlated either spatially or among the various fields, contribute to the off-diagonal terms. Preliminary experiments to determine the effects of measurement error on optimal sensor positioning have been conducted for relative errors of 5%, 10% and 15%. The results thus far are inconclusive with no trends in positioning found for various amounts of error in either the univariate or multivariate cases.

5. Summary

A demonstration of the capabilities of a multivariate sensor placement methodology has been given. It was shown, through the use of simulated data and their associated correlation functions, that objective analyses derived from observations taken at the optimal sampling points given by the placement algorithm were more accurate in the sense of having a smaller mean and variance of interpolation error than analyses derived from subjectively chosen sampling points. Demonstrations were given to show the methodology's ability to add sampling points optimally to existing networks and to place sampling points optimally when specified regions of the analysis grid are not admissible as sampling locations.

The results shown here suggest that the multivariate sensor placement algorithm could be useful in the design of field programs and data acquisition experiments. Interpretations of these results, however, must always consider the possibility that the nonlinear programming algorithm may have converged to a local rather than global minimum. Several runs of the algorithm with different starting vectors can aid in identifying solutions associated with local minima.

Research is currently underway to determine the effect of observational error on sensor placement. Future work will apply the sensor placement methodology to the design of mesoscale networks and optimal sampling strategies for remote sensors such as radars. Since the optimization problem becomes large with increasing numbers of sensors and larger grid sizes, improvements in the methodology will concentrate on vectorizable optimization algorithms that can take advantage of currently available supercomputers.

Acknowledgments. The author wishes to acknowledge Professor J. J. Stephens, Florida State University, for his many helpful suggestions during the course of this research. Portions of this research were conducted with the support of the Supercomputer Computations Research Institute, which is partially funded by the U.S. Department of Energy through Contract DE-FC05-85ER250000.

APPENDIX

Derivation of Analytic Fields

The multivariate analytic model used to simulate atmospheric fields employed the geostrophic wind equations to derive functional forms of the wind component fields from a specified function representing geopotential. The specification of certain variables within the model as random variables with defined probability density functions enables the determination of the associated spatial covariances and cross covariances.

Consider the analytic function representing the geopotential at point (x_j, y_j):

$$\Phi_j = \Phi(x_j, y_j) = A \cos(\omega_x X_j) \cos(\omega_y Y_j) - BY_j \quad \text{(A1)}$$

where

$$X_j = x_j - x_c,$$

$$Y_j = y_j - y_c,$$

(x_j, y_j) = coordinates of the jth point,

$$\omega_x = \frac{2\pi}{l_x}, \quad \omega_y = \frac{2\pi}{l_y},$$

(x_c, y_c) is the origin of the system, and ω_x and ω_y are radian wavenumbers in the x and y directions, with associated wavelengths l_x and l_y.

Let A, B, ω_x and ω_y be random variables with independent normal distributions such that

$$A \sim N(a, \sigma_a^2),$$
$$B \sim N(b, \sigma_b^2),$$
$$\omega_x \sim N(\mu_x, \sigma_x^2),$$
$$\omega_y \sim N(\mu_y, \sigma_y^2).$$

The probability distribution functions for A, B, ω_x and ω_y are, respectively,

$$p_A(A) = \frac{1}{\sqrt{2\pi}\sigma_a} \exp\left[-\frac{(A-a)^2}{2\sigma_a^2}\right]; \quad -\infty \leq A \leq \infty, \tag{A2}$$

$$p_B(B) = \frac{1}{\sqrt{2\pi}\sigma_b} \exp\left[-\frac{(B-b)^2}{2\sigma_b^2}\right]; \quad -\infty \leq B \leq \infty, \tag{A3}$$

$$p_{\omega_k}(\omega_k) = \frac{1}{\sqrt{2\pi}\sigma_k} \exp\left[-\frac{(\omega_k-\mu_k)^2}{2\sigma_k^2}\right]; \quad -\infty \leq \omega_k \leq \infty; \quad k = x, y. \tag{A4}$$

The expected value of Φ at point (x_j, y_j) is

$$E[\Phi_j] = E[A]E[\cos(\omega_x X_j)]E[\cos(\omega_y Y_j)] - E[B]Y_j,$$
$$= a\cos(\mu_x X_j)\exp\left(-\tfrac{1}{2}\sigma_x^2 X_j^2\right) \times \cos(\mu_y Y_j)\exp\left(-\tfrac{1}{2}\sigma_y^2 Y_j^2\right) - bY_j, \tag{A5}$$

where the expected value operator, E, is defined for a function of a random variable, ξ, with a probability distribution function, p, as

$$E[\xi] = \int_{-\infty}^{\infty} f(\xi) p_\xi(\xi) d(\xi). \tag{A6}$$

Similarly, expressions for the expected value of the u and v fields can be derived. They are, respectively,

$$E[u_j] = \frac{1}{f_j}\{E[A]E[\cos(\omega_x X_j)]E[\omega_y \sin(\omega_y Y_j)] + E[B]\},$$
$$= \frac{1}{f_j}\left\{a\cos(\mu_x X_j)\exp\left(-\tfrac{1}{2}\sigma_x^2 X_j^2\right) \times [\mu_y \sin(\mu_y Y_j) + \sigma_y^2 Y_j \cos(\mu_y Y_j)]\exp\left(-\tfrac{1}{2}\sigma_y^2 Y_j^2\right) + b\right\}, \tag{A7}$$

and

$$E[v_j] = -\frac{1}{f_j}\{E[A]E[\omega_x \sin(\omega_x X_j)]E[\cos(\omega_y Y_j)]\},$$
$$= -\frac{a}{f_j}[\mu_x \sin(\mu_x X_j) + \sigma_x^2 X_j \cos(\mu_x X_j)] \times \exp\left(-\tfrac{1}{2}\sigma_x^2 X_j^2\right)\cos(\mu_y Y_j) \times \exp\left(-\tfrac{1}{2}\sigma_y^2 Y_j^2\right). \tag{A8}$$

The cross covariance between two random variables is defined as

$$\text{ccvf}[\xi_j, \eta_k] = E[\xi_j \eta_k] - E[\xi_j]E[\eta_k] \tag{A9}$$

where ξ_j and η_k are functions of random variables evaluated at points j and k, respectively. The autocovariance of a function of random variables between points j and k is

$$\text{acvf}[\xi_j, \xi_k] = E[\xi_j \xi_k] - E[\xi_j]E[\xi_k]. \tag{A10}$$

The use of (A9) and (A10) enables the computation of the spatial covariances associated with the analytic fields. The equations expressing the variance result when $j = k$ in (A10). For Φ, u and v at point (x_j, y_j) they are, respectively,

$$\text{Var}[\Phi_j] = \tfrac{1}{4}(\sigma_a^2 + a^2)[1 + \cos(2\mu_x X_j)\exp(-2\sigma_x^2 X_j^2)] \times [1 + \cos(2\mu_y Y_j)\exp(-2\sigma_y^2 Y_j^2)] + \sigma_b^2 Y_j^2 - \frac{a^2}{4}[1 + \cos(2\mu_x X_j)]\exp(-\sigma_x^2 X_j^2) \times [1 + \cos(2\mu_y Y_j)]\exp(-\sigma_y^2 Y_j^2), \tag{A11}$$

$$\text{Var}[u_j] = \frac{1}{f_j^2}\left(\tfrac{1}{4}(\sigma_a^2 + a^2)[1 + \cos(2\mu_x X_j) \times \exp(-2\sigma_x^2 X_j^2)] \times \{(\sigma_y^2 + \mu_y^2) - [(-4\sigma_y^4 Y_j^2 + \sigma_y^2 + \mu_y^2)\cos(2\mu_y Y_j) - 4\mu_y \sigma_y^2 Y_j \sin(2\mu_y Y_j)] \times \exp(-2\sigma_y^2 Y_j^2)\} - a^2 \cos^2(\mu_x X_j)\exp(-\sigma_x^2 X_j^2) \times [\mu_y^2 \sin^2(\mu_y Y_j) + 2\mu_y \sigma_y^2 Y_j \sin(\mu_y Y_j)\cos(\mu_y Y_j) + \sigma_y^4 Y_j^2 \cos^2(\mu_y Y_j)]\exp(-\sigma_y^2 Y_j^2) + \sigma_b^2\right), \tag{A12}$$

and

$$\text{Var}[v_j] = \frac{1}{f_j^2}\left(\tfrac{1}{4}(\sigma_a^2 + a^2)\{(\sigma_x^2 + \mu_x^2) - [\cos(2\mu_x X_j) \times (-4\sigma_x^4 X_j^2 + \sigma_x^2 + \mu_x^2) - 4\mu_x \sigma_x^2 X_j \sin(2\mu_x X_j)] \times \exp(-2\sigma_x^2 X_j^2)\} \times [1 + \cos(2\mu_y Y_j) \times \exp(-2\sigma_y^2 Y_j^2)] - a^2[\mu_x^2 \sin^2(\mu_x X_j) + 2\mu_x \sigma_x^2 X_j \times \sin(\mu_x X_j)\cos(\mu_x X_j) + \sigma_x^4 X_j^2 \cos^2(\mu_x X_j)] \times \exp(-\sigma_x^2 X_j^2) \times \cos^2(\mu_y Y_j)\exp(-\sigma_y^2 Y_j^2)\right). \tag{A13}$$

The autocorrelation function of a particular field is obtained by dividing the autocovariance function by the appropriate expression for standard deviation for that field, e.g.,

$$\mathrm{acf}[\Phi_j, \Phi_k] = \frac{\mathrm{acvf}[\Phi_j, \Phi_k]}{\sqrt{\mathrm{Var}[\Phi_j]}\sqrt{\mathrm{Var}[\Phi_k]}}. \qquad \text{(A14)}$$

The cross-correlation function between two fields is obtained by dividing the cross-covariance function by the two appropriate standard deviations, e.g.,

$$\mathrm{ccf}[\Phi_j, u_k] = \frac{\mathrm{ccvf}[\Phi_j, u_k]}{\sqrt{\mathrm{Var}[\Phi_j]}\sqrt{\mathrm{Var}[u_k]}}. \qquad \text{(A15)}$$

REFERENCES

Alaka, M. A., and F. Lewis, 1967: Numerical experiments leading to the design of optimum global meteorological networks. Tech. Memo. WBTM TDL-7, ESSA, Weather Bureau, Washington DC, 14 pp.

——, and R. C. Elvander, 1972a: Optimum interpolation from observations of mixed quality. *Mon. Wea. Rev.*, **100,** 612–624.

——, and ——, 1972b: Matching of observation accuracy and sampling resolution in meteorological data acquisition experiments. *J. Appl. Meteor.*, **11,** 567–577.

Bretherton, F. P., and J. C. McWilliams, 1980: Estimations from irregular arrays. *Rev. Geophys. Space Phys.*, **18,** 789–812.

Buell, C. E., 1960: The structure of two-point wind correlations in the atmosphere. *J. Geophys. Res.*, **65,** 3353–3366.

——, 1972: Correlation functions for wind and geopotential on isobaric surfaces. *J. Appl. Meteor.*, **11,** 51–59.

Eddy, G. A., 1973: The objective analysis of atmospheric structure. *J. Meteor. Soc. Japan,* **51,** 450–457.

——, 1974: An approach to the design of meteorological field experiments. *Mon. Wea. Rev.*, **102,** 702–707.

Fujioka, F. M., 1986: A method for designing a fire weather network. *J. Atmos. Oceanic Technol.*, **3,** 564–570.

Gandin, L. S., 1963: *Objective Analysis of Meteorological Fields.* Translated from Russian by Israel Program for Scientific Translations, Jerusalem, 1965, 242 pp. [NTIS TT65-50007.]

——, 1970: The planning of meteorological station networks. WMO Tech. Note No. 111, Geneva, 35 pp.

——, S. Mashkovich, M. Alaka and F. Lewis, 1967: Design of optimum networks for aerological observing *stations.* WWW Planning Rep. No. 21, WMO, Geneva, 58 pp.

Himmelblau, D. M., 1972: *Applied Nonlinear Programming.* McGraw-Hill, 498 pp.

Husain, T., and M. Ukayli, 1982: Meteorological network expansion for Saudi Arabia. *J. Rech. Atmos.*, **16,** 281–294.

——, —— and H. U. Khan, 1984: Evaluation of meteorological network of Saudi Arabia using information theory. *J. Meteor. Soc. Japan,* **62,** 783–790.

——, —— and ——, 1986: Meteorological network expansion using information decay concept. *J. Atmos. Oceanic. Technol.*, **3,** 27–35.

Huss, A., 1971: On the introduction of space–time correlation functions in optimum objective analysis methods. *J. Appl. Meteor.*, **10,** 152–155.

Julian, P. R., and H. J. Thiebaux, 1975: On some properties of correlation functions used in optimal interpolation schemes. *Mon. Wea. Rev.*, **103,** 605–616.

Kasahara, A., 1972: Simulation experiments for meteorological observing systems for GARP. *Bull. Amer. Meteor. Soc.*, **53,** 252–264.

——, and D. Williamson, 1972: Evaluation of tropical wind and reference pressure measurements: Numerical experiments for observing systems. *Tellus,* **24,** 100–115.

Myach, L. T., and O. Sirotenko, 1973: Efficient placement of meteorological stations as a problem of operations research. *Meteor. Hydrol.*, **3,** 43–53.

Schlatter, T. W., 1975: Some experiments with a multivariate statistical objective analysis scheme. *Mon. Wea. Rev.*, **103,** 246–257.

Seaman, R. S., 1977: Absolute and differential accuracy of analyses achievable with specified observational network characteristics. *Mon. Wea. Rev.*, **105,** 1211–1222.

Shannon, C. E., and W. Weaver, 1949: *Mathematical Theory of Communication.* University of Illinois Press, 125 pp.

Thiebaux, H. J., 1973: Maximally stable estimation of meteorological parameters at grid points. *J. Atmos. Sci.*, **30,** 1710–1714.

——, 1975: Experiments with correlation representations for objective analysis. *Mon. Wea. Rev.*, **103,** 617–627.

Yerg, M. C., 1973a: A systems approach to optimal experimental design in meteorology. University of Oklahoma, Department of Meteorology Report, 110 pp.

——, 1973b: An optimal sampling and analysis methodology. University of Oklahoma, Department of Meteorology Report, 70 pp.